A long-term study of the collective cell behavior of phytoplankton using the moment approximation method of an individual-based model (IBM).

Bordj. N[1,3] and El Saadi. N[1,2]

[1] Laboratoire de Modélisation de Phénomènes Stochastiques (LAMOPS), ENSSEA, Algiers, Algeria
[2] Ecole Nationale Supérieure de Statistique et dÉconomie Appliquée (ENSSEA), Algiers, Algeria
[3] University Algiers 3, FSCESG, Algiers, Algeria

Abstract. The objective of this work is to analyse the ability of a spatial moment model (SMM) to approximate an individual-based model (IBM) dedicated to the study of the aggregation phenomenon in a mobile phytoplankton population. The dynamic system of spatial moments is a system of integro-differential equations derived from a phytoplankton IBM. The later is built on the basis of stochastic processes describing the dynamics of phytoplankton cells and their interactions. These processes are the movement of cells which takes into account the random dispersion of cells in water and the attraction between cells due to their chemosensory abilities, and the branching process (cell division or cell death) in which the effect of local competition for nutrient resources on the cells division process is taken into account through the use of density dependent division rate.
We solve numerically the SMM and then simulate the two models (IBM and SMM) for to analyze the aggregation in the population. The numerical results have led to the conclusion that in contrast to the meanfield model (MFM), the method of spatial moments is efficient to capture the dynamics of the IBM. Further, the SMM easily permits the prediction of long term behavior of phytoplankton cells and their spatial structure.
Regardless of competition intensity, in the long term the population tends to be stable with formation of aggregates, as a result of the equilibrium between different mechanisms, including reproduction, competition, diffusion and cells attractions due to chemosensory abilities.

Keywords: Individual-based model · Spatial moment dynamics · Integro-differential equations system · Numerical method and simulation · spatial and temporel discretization · Phytoplankton aggregation.

1 Introduction

Individual-based models (IBM), are simulation models that treat individuals as unique, discrete entities [14], taking into account all the particularities and details judged essential to these entities. Thus, these models permit to describe, at the microscopic level, the behaviours of individuals and their interactions, in order to observe the global evolution

of the system. However, given the details contained in these IBM, the latter can be very complex, computationally intensive and, moreover costly in time and memory during their simulation. Simpler models than IBM exist, they are called Eulerian (aggregate) models or mean-field models. These models, in contrast with the IBM, represent a system as a whole, at the macroscopic level, assuming the behavioural and environmental homogeneity of the studied populations. Therefore, as soon as there is heterogeneity in the spatial structure (aggregations or concentrations in space), these models become inappropriate.

A new approach considered the middle ground between oversimplified mean-field models and highly complex computer simulation models, has been recently developed. It is called the spatial moments method or moment closure method [3, 4, 7, 17, 19–22]. This method represents a good tool to reduce the complexity of an IBM, it allows to build deterministic models, by approximating the dynamics of an IBM with a mathematical model, aggregated and simpler, taking into account the main individuals characteristics and their spatial structure and capturing the effects of interactions and movements of individuals at the local level and in small neighborhoods. So, moment approximation helps to minimize computation time and facilitates understanding of events.

This paper aims to present a new application of the spatial moments method in a marine ecological system. Further, we attempt to assess the capacity of this method in approximating individual-based models through the study of the aggregation behavior in a phytoplankton population.

Phytoplankton includes all the unicellular microalgae living in suspension in the water, most often in the form of a ”patch”, due to their aggregative nature which allows them to aggregate and stick together to form relatively large particles. This is due to their aggregative nature which allows them to aggregate and stick together to form relatively large particles called aggregates. Small-scale biological studies have shown the existence of interactions and biological responses between phytoplankton cells. In fact, some mobile phytoplankton species, such as algae and dinoflagellates, possess chemosensory abilities that allow them to sense the presence of other phytoplankton cells if they are in their vicinity. Indeed, these phytoplanktonic species, after the completion of photosynthesis, evacuate organic matter into the water. The extracellular products such as amino acids and sugars create a highly concentrated zone around the phytoplankton cell called the *phycosphere*. [2, 15]. This zone, with a very high concentration of excreted products, extends over several diameters of the surface of the cell and creates a chemical field around it that has an attractive effect on the algal cells and bacteria situated in its immediate vicinity.

So, for a good description of phytoplankton population dynamics and a better understanding of the interactions and mechanisms that govern it, it is utile to pass from the population scale to the individual scale (individual-based modelling).

The goal of our work is to analyse at the long-term the spatial structure of a phytoplankton population using moment approximation method of an individual-based model. We first develop an IBM (at the microscopic scale) describing the stochastic processes of birth, death and movement of phytoplankton cells. This IBM extends El Saadi's IBM model [9–12] through the introduction of the local competition on resources in the division process, where we consider that the rate of division of each cell

depends on the local density of the individuals surrounding it [8]. Also, the model takes into account interactions between phytoplankton cells due to their chemosensory abilities in the movement process. We then approximate the obtained IBM using the spatial moment method (at the mesoscopic scale), and determine the dynamic equations of the first spatial moment (which is the average density of individuals in the system) and the second spatial moment (which is the average density of pairs of individuals providing information on the spatial structure of the population). After solving numerically the spatial moment model (SMM), we simulate both the IBM and SMM, in order to compare their results and to see if the spatial moment dynamic equations are really efficient to approximate the IBM model, and whether it can predict the long-term behavior of phytoplankton cells and their spatial structure.

2 Individual-Based Model

We describe an individual based model (IBM) for a population of mobile phytoplankton undergoing movement and branching (cell birth and death).

Let us consider a finite population of phytoplankton cells, randomly distributed in a two dimensional and continuous space $L \times L$. The phytoplankton cells are considered as points of particles represented by their localizations x. At time t, each cell i is located at coordinate $x_i(t) = (x_{i1}(t), x_{i2}(t))$, $i = 1, ..., n(t)$, where $n(t)$ is the number of phytoplankton cells at time t and the vector $\big(x_1(t), ..., x_{n(t)}(t)\big)$defines the spatial structure $p(x, t)$ at that time t, which changes through the occurrence of the stochastic processes of movement, division and death.

- ***The motion process***

The spatial movement of the cells in the space depends on their positions. For a given cell i located in $x_i(t)$, at time t, its displacement is defined by the following stochastic differential equation [1, 9–12]:

$$dx_i(t) = \sum_{j=1, j\neq i}^{n(t)} \alpha\, F(x_i(t) - x_j(t))dt + \sqrt{2Df}\, dB_i(t) \qquad i = 1, ..., n(t) \quad (1)$$

The first term on the right represents the pair interactions between the cell i and the other cells of the system, the second term represents the random force acting on the particle i, which is the diffusion of this cell in water, where Df represents the diffusion coefficient of a cell in the water and $(B_i(t))_t$ is a standard Wiener process with values in $\mathbb{R}^2$. $\sum_{j=1, j\neq i}^{n(t)} \alpha\, F(x_i(t) - x_j(t))$ measures the influence of all the other cells in the system located in $x_j(t)$ on the cell i located in $x_i(t)$ due to their chemosensory capacities (we consider in the following $x_i(t) = x_i$ and $x_j(t) = x_j$). Indeed, after the completion of photosynthesis, the extracellular products released by a phytoplankton cells at a position x_i, form a concentration field around it on a radius of length r_0 ($r_0 \succ 0$). This field attracts all the cells that are at positions x_j, such that the distance $\| x_i - x_j \|$ is between r_0 and r_1, where r_1 represents the maximum distance beyond which individuals are

unable to detect their congeners, with $(r_1 \succ r_0)$ and r_0, r_1 are the non-negative reals that delimit the sensitivity interval in phytoplankton cells. For any pair of cells located in x_i and x_j, the interaction is defined by: $\alpha F(x_i - x_j)$, with α the mass of a phytoplankton cell and $F(x_i - x_j)$ is a kernel of attraction:

$$F(x_i - x_j) = -\frac{(x_i - x_j)}{\| x_i - x_j \|}\left[-\| x_i - x_j \|^2 + (r_0 + r_1) \| x_i - x_j \| - r_0 r_1\right] \times 1_{]r_0, r_1[}(\| x_i - x_j \|).$$

$F(x_i - x_j)$: represents a force that attracts the cell located in x_i to the one being in x_j, is a function of distance $\| x_i - x_j \|$, of magnitude $\left[-\| x_i - x_j \|^2 + (r_0 + r_1) \| x_i - x_j \| - r_0 r_1\right] 1_{]r_0, r_1[}(\| x_i - x_j \|)$, which increases in the interval $]r_0, r_1[$, peaked in $(\frac{r_0 + r_1}{2})$ and then decreases to 0 in r_1. Its direction vector is $-\frac{(x_i - x_j)}{\|x_i - x_j\|}$. Moreover, F is an odd function and symmetrical, so that, if the individual in x_i is attracted by the individual in x_j, then the individual in x_j is also attracted by the individual x_i [9].

As we attempt in the next step to approximate the IBM and pass to the macroscopic scale, then from the motion equation in (Eq. 1) given at the microscopic scale with the assumption that the population size $n(t)$ is finite, we deduce the probability of motion of a cell located in x_i in space to another location x, in case the population size becomes infinite (macroscopic scale). This transition probability will be expressed by the probability density function $m(x - x_i)$ such that:

$$m(x - x_i) = \frac{1}{4\pi D f \triangle_t} \exp\left\{-\frac{1}{4 D f \triangle_t}\left|\left|x - x_i - \int \alpha F(x_i - x_j) \triangle_t dx_j\right|\right|^2\right\} \; x,\, x_i,\, x_j \in L^2 \tag{2}$$

where $m(x - x_i)$ is a gaussian motility kernel. (Eq. 2) is obtained from (Eq. 1). $\triangle_t$ is the time step and the term $\int \alpha\, F(x_i - x_j)\, \triangle_t\, dx_j$ measures the effect of all cells of the system located in x_j on the cell i located in x_i, following their chemosensory capabilities. $|m|$ represents the total probability of movements' cell i [8], and measuring the set of possible displacements of the cell , such that $|m| = \int m\,(\xi)\, d\xi$ with $\xi = x - x_i \neq 0$.

- ***The birth process***

A phytoplankton cell i located at $x_i = (x_{i1}, x_{i2})$ has the probability (per unit of time) $B(x_i)$ of producing a newborn at the same place where it is. This probability is defined by:

$$B(x_i) = b_1 - b_2\, d_{loc}(x_i) \tag{3}$$

where b_1 and b_2 are the density-independent and the density dependent division rates respectively. The term $b_2\, d_{loc}(x_i)$ modifies the division rate, following the hypothesis of existence of competition between phytoplankton cells for nutrient resources [8, 17]. $d_{loc}(x_i)$ is the local density of individuals in x_i, the term $b_2\, d_{loc}(x_i)$ measures the effect of all nearby individuals, surrounding the x_i cell and causing a diminution in the division rate. So, increasing the local density of phytoplankton cells reduces the

food level and consequently decreases the reproduction rate of this population. The local density $d_{loc}(x_i)$ is defined by:

$$d_{loc}(x_i) = \int w(x_j - x_i)\ [p(x_j, t) - \delta_{x_i}(x_j)]\ dx_j \tag{4}$$

with

$$w(x_j - x_i) = \frac{1}{q} \exp\left\{-\frac{\|x_j - x_i\|^2}{2s_w^2}\right\} \quad \& \quad p(x_j, t) = \sum_{k=1}^{n(t)} \delta_{x_j}(x_k)$$

$w(x_j - x_i)$ represents the competition kernel, which measures the contribution of individuals j located at x_j in the local density perceived by an individual located in x_i. This kernel is a function of the distance, is Gaussian, symmetric and normalized to 1, such that $\int w(\xi)d\xi = 1$. This type of kernel has been chosen to give greater weight to the nearest neighbors. s_w is the width of competition kernel and $1/q$ the normalization constant. $p(x_j, t)$ is the local density of individuals in x_j and $\delta_{x_i}(x_j)$ is the Dirac delta function, to remove the effect of individual located in x_i for the calculation of $p(x_j, t)$, because it can't compete with itself [8, 17].

- ***The death process***

The probability (per unit time) that the cell located in $x_i = (x_{i1}, x_{i2})$ dies, is constant and is given by :

$$D(x_i) = d \tag{5}$$

3 Spatial Moment Model

Dynamic systems of spatial moments are constructed from stochastic processes of birth, death and movement of individuals [4, 8, 17, 20]. The moment-based approximation helps to understand the phenomena by describing the spatial structure through statistics that summarise its main characteristics and describe the population dynamics. For a spatial structure $p(x, t)$ at time t, these statistics are: **the first spatial moment** $\mathbf{N}(\mathbf{t})$ which corresponds to the average density of individuals over the whole space ($L \times L$), **the second spatial moment** $\mathbf{C}(\xi, \mathbf{t})$ defined as the average density of pairs of individuals separated by a distance ξ and which provides information on how the individuals are distributed in the $L \times L$ space, and **the third spatial moment** $\mathbf{T}(\xi, \xi', \mathbf{t})$ considered as a closure moment and which corresponds to the density of triplets formed by the first pair of individuals separated by a vector distance ξ and a third individual separated from the first pair by a vector distance ξ'.

During the realisations of stochastic processes in our presented IBM, spatial moments take new values each time the spatial structure changes. Thus, on average the first two moments will change over time according to the following differential equations:

- ***The dynamics of the first moment*** is given by:

$$\frac{dN(t)}{dt} = (b_1 - d)N(t) - b_2 \int w(\xi)C(\xi,t)d\xi \tag{6}$$

The term $(b_1-d)N(t)$ corresponds to the population growth resulting from the components of independent neighborhood division and death. The second term $b_2 \int w(\xi)C(\xi,t)d\xi$ represents the neighborhood-dependent division component and measures the negative effect that the local environment may have on reproduction and population growth as a consequence of competition on resources between individuals. If we put $C(\xi,t) = N^2(t)$ in , then the spatial heterogeneity is eliminated and we obtain the Lotka Volterra dynamics of the mean-field theory:

$$\frac{dN(t)}{dt} = (b_1 - d)N(t) - b_2 N^2(t) \tag{7}$$

- ***The dynamics of the second spatial moment*** is given by:

$$\frac{dC(\xi,t)}{dt} = \left(\frac{dC(\xi,t)}{dt}\right)_{Division} + \left(\frac{dC(\xi,t)}{dt}\right)_{Death} + \left(\frac{dC(\xi,t)}{dt}\right)_{Movement}$$

The spatial structure of pairs of cells, separated with a vectorial distance ξ, changes through the division, death and movement stochastic processes. Hence, the dynamics of the spatial second moment, take into account all the events that can affect individuals of a pair:

$$\begin{aligned}
&\frac{dC(\xi,t)}{dt} = \\
&Birth \quad \begin{cases} 2b_1C(\xi,t) - 2b_2w(\xi)C(\xi,t) \\ -b_2 \int w(\xi')T(\xi,\xi',t)\, d\xi' \\ -b_2 \int w(\xi')T(-\xi,\xi',t)\, d\xi' \\ +b_1^2C(\xi,t) - b_2^2w^2(\xi)C(\xi,t) \\ -b_2^2 \int\ w(\xi')w(\xi'-\xi)T(\xi',\xi'-\xi,t)\, d\xi' \end{cases} \\
&\quad + \\
&Death \quad \{\ -2dC(\xi,t) - d^2C(\xi,t) \\
&\quad + \\
&Movement \ \begin{cases} -2\,|m|\ C(\xi,t) + 2\int m(\xi')C(\xi+\xi',t)\, d\xi' \\ +\int\ m(\xi')m(-\xi'')C(\xi+\xi'-\xi'',t)\, d\xi'\, d\xi'' \end{cases}
\end{aligned} \tag{8}$$

The terms to the right of the equation (Eq. 8), count the new pairs of individuals separated by a distance ξ which will be created: either by cell movement, or by reproduction cell of one of the two phytoplankton cells composing a given existing pair or by the simultaneous reproduction of the two cells which compose it, while taking into account the negative effect of competition caused by all neighboring individuals and reducing the cell reproduction of individuals forming a pair as well as the loss of pairs separated by a distance ξ due to movement or the death of one of the individuals or of the two individuals composing these pairs (for more details, see [5]).

We note that in the dynamic system of spatial moments composed by equations (eq. 6) and (eq. 8), that the dynamics of each spatial moment depends on the higher order moment. To avoid these dependencies and to close the system, we will express the third spatial moment in terms of the first and second spatial moments. This expression is called the closure moment [8, 20].

4 Numerical methods and simulations

We simulate the IBM using the Gillespie algorithm [13], which is a procedure for numerical simulation of the temporal evolution of the stochastic system, allowing to specify when the next event will occur, which events will be and who is the individual concerned by this event (for more details, see [5]).

For the analysis of the IBM results and their comparison with those of the spatial moment model, it is necessary to calculate the first spatial moment and the Clark & Evans index after each realization of the individual-based model.

– **The first spatial moment** $N(t)$ which represents the average density of the individuals, is obtained by dividing the total number of cells $n(t)$ within a population at the time t by the area of the domain $|L|^2$ (with $|L|$ the domain length):

$$N(t) = \frac{n(t)}{|L|^2} \tag{9}$$

– **The Clark & Evans index** I_{CE} also called the nearest neighbor method [6], allowing to analyze the aggregation of individuals in a given space, is defined by:

$$I_{CE} = \frac{\bar{r}_a}{\bar{r}_e} \tag{10}$$

with

$$\bar{r}_a = \frac{1}{n(t)} \sum_{i=1}^{n(t)} r_i \quad \& \quad \bar{r}_e = \frac{1}{2\sqrt{N(t)}}$$

where, $\bar{r}_a$ represents the average of distances to nearest neighbor, $\bar{r}_e$ is the average distance to nearest neighbor expected in an infinitely large random distribution, and r_i is the nearest neighbor's distance from the individual i. If $I_{CE} = 1$, then the spatial structure is random; If $I_{CE} < 1$, then it is aggregated (in the case of an extreme aggregation, $I_{CE} = 0$); And if $I_{CE} > 1$, the spatial structure is regular.

The dynamic model of the spatial moments obtained is a dynamic system of integro-differential equations, depending on the vector distance ξ and the time t. Its resolution is based on numerical methods allowing its temporal and spatial discretization. The trapezoid method is used to approximate the spatial integrals, and the explicit Runge Kutta method $(ode23)$ is used for the determination of the hierarchical moments, which allows to have, the values of the vector $N(t)$ representing the first spatial moment, as well as, the values of the symmetric matrix $C(\xi, t)$ (see, Fig. 2b) representing the

Table 1. Simulation parameters.

Descriptions	Symbols	Values	Units
Spatial Domain	$L \times L$	$[-100, 100] \times [-100, 100]$	μm^2
Initial cells density	$N(0)$	0.0156	$Cells.\mu m^-2$
Neutral Zone Limit	r_0	5	μm
Perception zone limit	r_1	45	μm
Mass of a phyto cell	α	0.04	$\mu m.day^{-1}$
Diffusion rate	Df	0.07	$\mu m^2.s^{-1}$
Independent division rate	b_1	$0,3$	day^{-1}
Dependent division rate	b_2	0.25	day^{-1}
Death rate	d	0.25	day^{-1}
Competition kernel width	sw	20	μm
Grid spacing	h	2	μm
Maximum simulation time	T_{max}	67	day

second spatial moment (the average density of the pairs of cells separated by a distance ξ at time t).

The spatial discretization of the vector distance $\xi = (\xi_1, \xi_2)$, was made through a grid spacing h, over the space. To obtain information about the spatial structure of our phytoplankton population from the spatial moments model, we compute the spatial correlation function (called, pair correlation function), denoted $C(r, t)$ by dividing the second spatial moment $C(\xi, t)$ by the square of the first spatial moment $N^2(t)$, where $r = \|\xi\| = \sqrt{\xi_1^2 + \xi_2^2}$ (Euclidean distance).

If the pair correlation function $C(r, t) = 1$, then there is absence of spatial structure (this is the case of the mean-field model); If $C(r, t) > 1$ for small values of r then it indicates an aggregated spatial structure; And, if $C(r, t) < 1$ then it indicates a disaggregated spatial structure [18].

We consider in this work only the case where $b_1 > d$, $b_2 > 0$ and the competition effect taken into account at the level of the birth process only reduces the creation of new pairs of individuals separated by a distance vector ξ but do not lead to its destruction, only the movement of cells or their death are responsible for the loss of even cells.

The figures below include the simulation results of the individual-based model (IBM), the spatial moments model (SMM) and the mean-field model (MFM), according to the parameter values summarized in the Table. 1. Moreover, for the model of spatial moments, we set as an initial condition at $t = 0$, $C(\xi, 0) = N^2(0)$ (corresponding to the absence of spatial structure). Regarding the IBM results presented in this work, each result is an average of 3 repetitions.

5 Results

5.1 The moment closure

For a good approximation of the IBM by the dynamic model of spatial moments, we must choose the appropriate moment closure for the third spatial moment. For this purpose, we compared the simulation results of the IBM with those obtained by the moments model in the case of using different closures: of power 1, of power 2 and of power 3. The different expressions of these closures are summarized in Appendix. A.

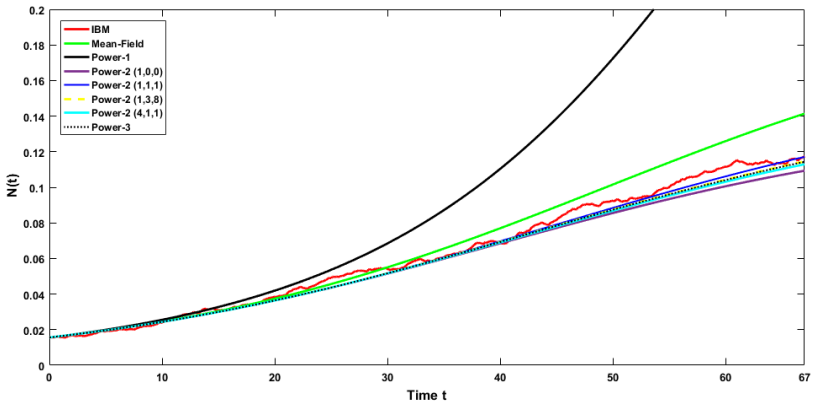

Fig. 1. *Comparison of moment closures for the third spatial moment. This graph represents the time evolution of the first spatial moment $N(t)$, obtained by simulating the IBM, MFM and the spatial moments model using six different closures whose expressions are defined in Appendix. A.*

The figure (Fig. 1) represents the time evolution of the first spatial moment $N(t)$, obtained by the IBM and the SMM when using six different closures. We note that the use of a symmetrical closure of power 2 with $\alpha = 1$, $\beta = 1$ and $\gamma = 1$ gives results for the SMM closer to those of the IBM, which leads to opt for the closure *power-2* $(1, 1, 1)$ and to use it in all simulations of the SMM.

5.2 The medium case

The figure (Fig. 2) shows the simulation of the spatial moments model and the mean-field model where all variable parameters take medium values. The graph (Fig. 2a) represents the temporal evolution of the average density of individuals $N(t)$ for a 300 $days$ duration in the case of SMM and MFM. For the spatial moments model, the $N(t)$ function grows at the beginning of the period corresponding to the population increase due to the cellular reproduction of phytoplankton. This growth induces the creation of aggregates which will be maintained thanks to the chemosensory capacities in phytoplankton cells, as shown in the figure (Fig. 2c) representing the time evolution of the pair correlation function for $r = 0$ in the case of the SMM, where the function C(0, t) grows and reaches a maximum value, indicating that aggregate formation attains a high level, coinciding with the top increase rate of N(t) (see, Fig. 2a, c). However, the $C(0, t)$ function subsequently decreases (see, Fig. 2c), since once important aggregates are formed, the local density of individuals increases and competition intensifies, which slows down cellular reproduction and thus the formation of aggregates till the density function of individuals $N(t)$ and the correlation function of pairs $C(0, t)$ achieve a stability (see, Fig. 2a, c), that indicates an aggregated spatial structure at equilibrium.

In the case of the mean-field model, the population undergoes logistic growth until attaining a stability (see, Fig. 2a) corresponding to the equilibrium density which is equal to $N^* = (b_1 - d)/b_2$. Notice that the graph of the $N(t)$ function has a lower

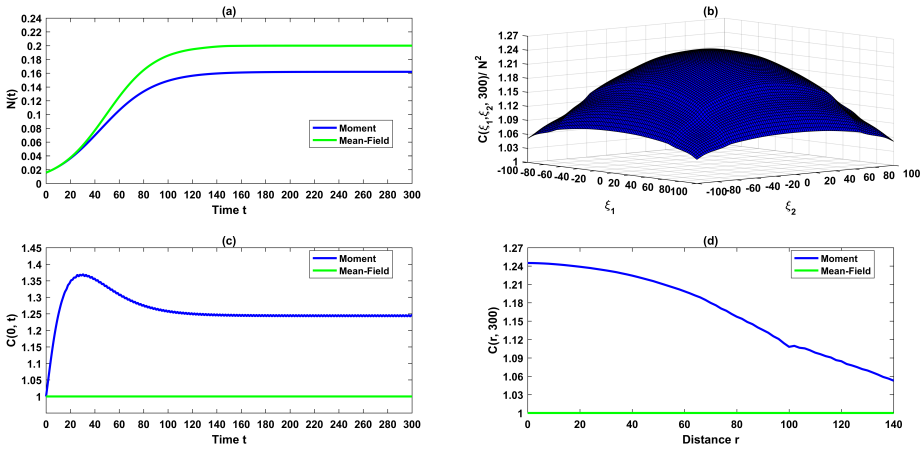

Fig. 2. *Simulation of the SMM and the MFM.* (a) *The first spatial moment as a function of time* t *expressed by the average density of individuals* $N(t)$ *for a period of* $300\ days$ *obtained by simulating the SMM and the MFM.* (b) *The pair correlation function at* $t = 300\ days$*, as a function of vector distance* $\xi = (\xi_1, \xi_2)$*, obtained by dividing the second spatial moment* $C(\xi, t)$ *at* $t = 300\ days$ *by* N^2 *at the same time* $t = 300\ days$*, using the SMM.* (c) *The temporal evolution of the pair correlation function* $C(r, t)$ *for* $r = 0$ *over a period of* $300\ days$ *in the case of the SMM and MFM.* (d) *The correlation function of pairs* $C(r, t)$ *as a function of distance* r *at time* $t = 300\ days$ *in the case of the SMM and MFM.*

level in the SMM than in the non-spatial model (MFM), because the moments model is dependent on the local density and takes into account the local spatial interactions that exist between phytoplankton cells (due to the competition on resources and attraction resulting from their chemosensory capacities), in contrast to the non-spatial model which considers the space homogeneous and ignores local effects of the spatial structure, so that, regardless of the variation in distance or time, the function $C(r, t)$ remains unchanged and equal to 1 (see, Fig. 2c, d).

The figure (Fig. 2b), which represents the pair correlation function at time $t = 300\ days$ as a function of the vector distance ξ, allows to see that the pair correlation function is a symmetrical function, with values greater than 1 indicating the existence of aggregates. Also, this function is a decreasing function with regard to distance, it takes high values when the vector distances between the individuals of a pair are narrow, i.e. when the individuals are aggregated. This is confirmed by the figure (Fig. 2d), which shows that the pair correlation function at time $t = 300\ days$ expressed as a function of the distance r (the Euclidean distance of ξ), is a decreasing function with distance r, and for $r = 0$, the pair correlation function takes its highest value.

The figure (Fig. 3), compares the simulation results of the IBM, SMM and MFM in the medium case where all variable parameters take medium values. We note that the first spatial moment $N(t)$ predicted by the IBM, is similar to the approximation given by the spatial moments model, both have the same trendendency (see, Fig. 3a). Concerning the spatial structure of the population, the results obtained by the IBM and the SMM show the transition from a regular spatial structure to an aggregated one. Indeed, according to the graphs (Fig. 3b, c) which respectively represent the temporal evolution for 67 $days$ of the Clark & Evans index I_{CE} and the pair correlation function $C(r, t)$

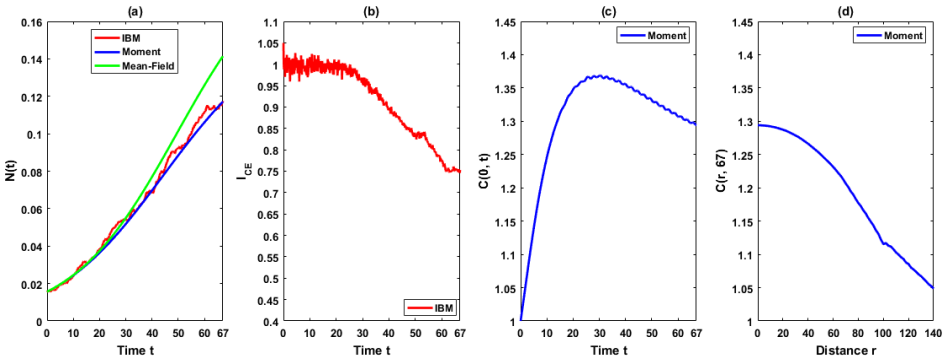

Fig. 3. *Simulation results of the IBM, the MFM and the SMM.* (a) *Represents the temporal evolution of the average density of individuals* $N(t)$ *for a duration of* $67\ days$*, obtained by the IBM, the SMM and the MFM.* (b) *The temporal evolution of the Clark & Evans index* (I_{CE}) *for* $67\ days$*, obtained by simulating the IBM.* (c) *The temporal evolution of the pair correlation function* $C(r,t)$ *for* $67\ days$ *in case* $r = 0$*, obtained by simulating the SMM.* (d) *Represents the evolution of the correlation function of pairs* $C(r,t)$ *as a function of distance* r *at* $t = 67\ days$*, obtained by the SMM.*

for $r = 0$, we see that at the beginning of the period of intense population reproduction and thus at the beginning of the creation of aggregates (see, Fig. 3a), the Clark & Evans index displays values varying approximately between 0.96 and 1.05 (see, Fig. 3b), while the $C(0,t)$ correlation function increases (see, Fig. 3c). The accentuation of aggregation, made that the function $C(0,t)$ continued to rise until it reached its peak, coinciding with a marked decrease in Clark & Evans index values, being less than 1, indicating the amplification and strengthening of aggregates within the population. But, since competition intensifies, there will then be a reduction in aggregate formation, expressed by the diminution of $C(0,t)$ and by the slowing down of the Clark & Evans index. The results obtained at the end of the period in $t = 67\ days$ reflect the existence of aggregates in the population (see, Fig. 3b, c, d), the I_{CE} index attains an approximate value of 0.75 and the $C(r,67)$ function which decreases with distance, has values greater than 1, such that the final value of $C(0,t)$ function in $t = 67\ days$ (see, Fig. 3c) corresponds to the first value of the function $C(r,67)$ for $r = 0$ (see, Fig. 3d).

5.3 The effect of cellular diffusion

Through the figure (Fig. 4), we will study the effect of cell diffusion on population dynamics and spatial structure. We simulate the models IBM, MFM and SMM in the case of low diffusion (see, Fig. 4 a, b, c, d) and in the case of high diffusion (see, Fig. 4 e, f, g, h). Simulation results of the two scenarios obtained from the IBM are in agreement with the ones obtained from the SMM.

In the case of a low diffusion, the pairs correlation function $C(r,t)$ takes values greater than one, but that are higher compared to its values in the case of medium and high cell diffusion, whether for $C(0,t)$ (see, Fig. 3c and Fig. 4c, g) or for $C(r,67)$ (see, Fig. 3d and Fig. 4d, h) when the distance r between individuals is small. This means that aggregation between individuals is stronger in the case of low diffusion than in the case of medium and high diffusion. This is confirmed by the Clark & Evans index,

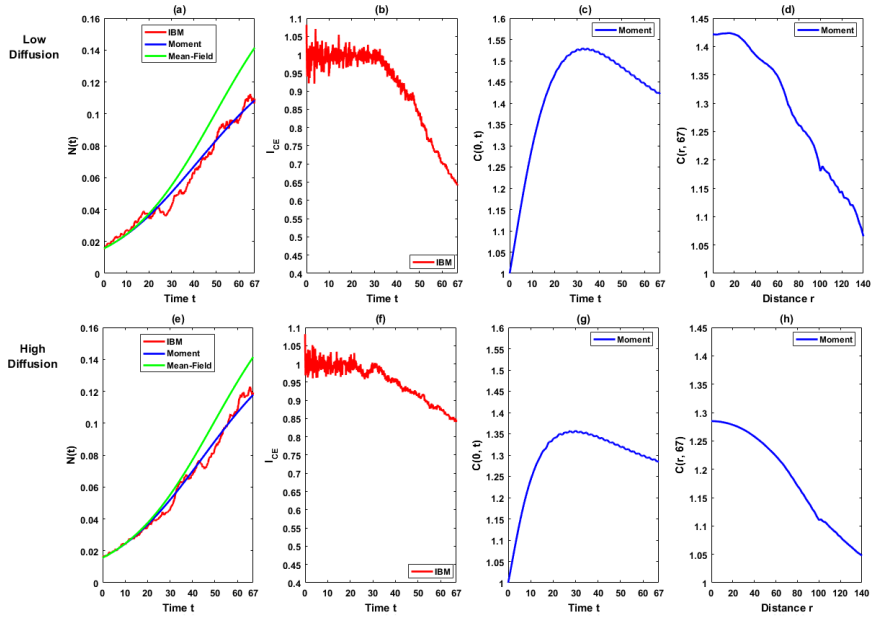

Fig. 4. *Analysis of the effect of cell diffusion using IBM, MFM and SMM. The graphs* $(a), (e)$ *Represent the temporal evolution of the average density of individuals* $N(t)$ *for a duration of* $67\ days$*, obtained by the IBM, the SMM and the MFM.* $(b), (f)$ *The temporal evolution of the Clark & Evans index* (I_{CE}) *for* $67\ days$*, obtained by simulating the IBM.* $(c), (g)$ *The temporal evolution of the pair correlation function* $C(r, t)$ *for* $67\ days$ *in case* $r = 0$*, obtained by simulating the SMM.* $(d), (h)$ *Represent the evolution of the correlation function of pairs* $C(r, t)$ *as a function of distance* r *at* $t = 67 days$*, obtained by the SMM. Graphs* $(a), (b), (c), (d)$ *are obtained in the case of low diffusion where* $Df = 0.04$*, and graphs* $(e), (f), (g), (h)$ *are obtained in the case of high diffusion where* $Df = 0.12$*, for the rest of the parameters take the same values (see, Table. 1).*

since the graph of I_{CE} shows values less than 1 and smaller in low diffusion than in medium and high diffusion (see, Fig. 3b and Fig. 4b, f). We also notice that the Clark & Evans index evolution concords with that of the function $C(0, t)$ (see, Fig. 4b, c, f, g). These results are explained by the fact that in case of weak diffusion, after phytoplankton reproduction, newborns move slowly and do not disperse rapidly from their mother cells, creating clusters of individuals that will maintain by the attraction process between cells due to the chemosensory competences. As the competition within these aggregates is medium, it acts by slowing down the birth rate, this leads to a reduction in the number and the sizes of the formed aggregates. As a result, the average density of individuals $N(t)$ is diminished in the case of low diffusion compared to the case of medium and high diffusion (see, Fig. 4a, e).

Inversely, when cell diffusion is high, cells tend to moving more rapidly in space, which does not facilitate the creation of aggregates, as shown in the graphs of $C(0, t)$ and $C(r, 67)$ in high diffusion (compared to the case of medium and low diffusion). This is also confirmed by the Clark & Evans index I_{CE}, which shows higher values in the case of high diffusion than in the case of medium and low diffusion. Thus the effect

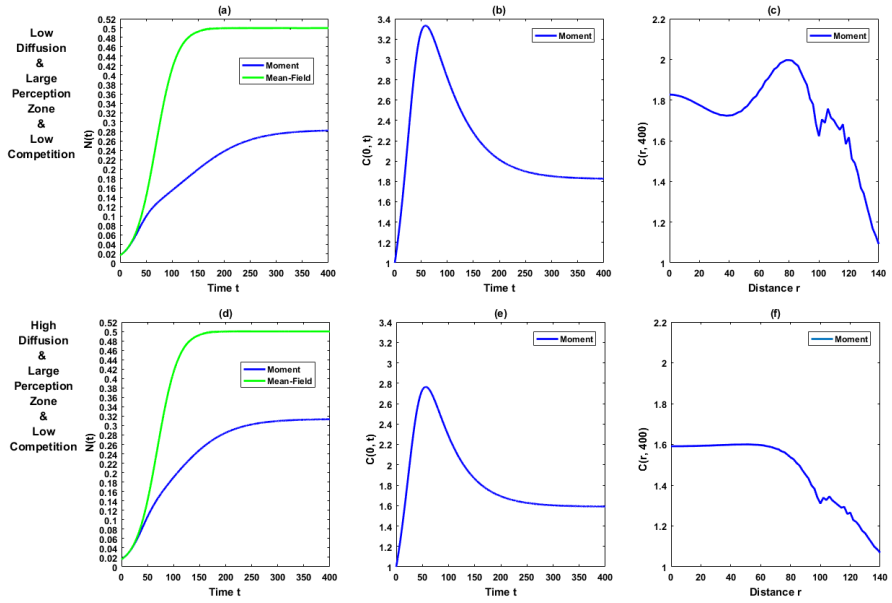

Fig. 5. *The simultaneous effect of competition and diffusion in the case of a large perception radius, using the SMM. The graphs* $(a), (d)$ *represent the first spatial moment as a function of time* t *expressed by the average density of individuals* $N(t)$ *for a period of* $400\ days$ *obtained by simulating the SMM and the MFM.* $(b), (e)$ *The temporal evolution of the pair correlation function* $C(r, t)$ *for* $400\ days$ *in case* $r = 0$*, obtained by simulating the SMM.* $(c), (f)$ *Represent the evolution of the pairs correlation function* $C(r, t)$ *as a function of distance* r *at* $t = 400\ days$*, obtained by the SMM. Graphs* $(a), (b), (c)$ *are obtained in the case where* $Df = 0.04$*,* $r_1 = 60$ *and* $b_2 = 0.1$*, and graphs* $(d), (e), (f)$ *are obtained in the case* $Df = 0.12$*,* $r_1 = 60$ *and* $b_2 = 0.1$*, for the rest of the parameters take the same values (see, Table. 1).*

of competition is reduced within the population, and as a result, the first spatial moment $N(t)$ in high diffusion reaches a higher level than in medium and low diffusion.

5.4 The simultaneous effect of cellular diffusion and competition over the long term

The figures (Fig. 5& Fig. 6) show at the long-term the simultaneous effect of cellular diffusion and competition on individual average density and on their aggregation in the case of a large perception radius, using the SMM. According to the obtained simulation results, a strong aggregation is found when diffusion and competition were simultaneously low (see, Fig. 5b compared to Fig. 5e & Fig. 6b, e). In fact, cellular reproduction under a weak competition between phytoplankton cells increases the density of individuals (see, Fig. 5a, d in comparison with Fig. 6a, d) and the creation of aggregates (see, Fig. 5b, e in comparison with Fig. 6b, e). Moreover, low cell diffusion favors the clustering of individuals and the appearance of dense aggregates (see, Fig. 5b), nevertheless the aggregation of individuals will continue until the competition within these clusters intensifies (following the increase in local density), causing a slowdown in cell

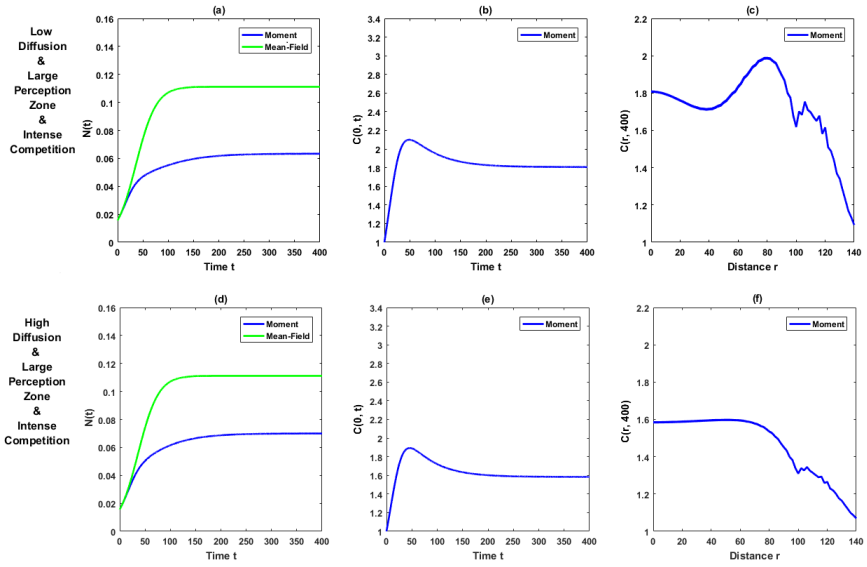

Fig. 6. *The simultaneous effect of competition and diffusion in the case of a large perception radius, using the SMM. The graphs* $(a), (d)$ *represent the first spatial moment as a function of time* t *expressed by the average density of individuals* $N(t)$ *for a period of* $400\ days$ *obtained by simulating the SMM and the MFM.* $(b), (e)$ *The temporal evolution of the pair correlation function* $C(r,t)$ *for* $400\ days$ *in case* $r = 0$*, obtained by simulating the SMM.* $(c), (f)$ *Represent the evolution of the pairs correlation function* $C(r,t)$ *as a function of distance* r *at* $t = 400\ days$*, obtained by the SMM. Graphs* $(a), (b), (c)$ *are obtained in the case where* $Df = 0.04$*,* $r_1 = 60$ *and* $b_2 = 0.45$*, and graphs* $(d), (e), (f)$ *are obtained in the case* $Df = 0.12$*,* $r_1 = 60$ *and* $b_2 = 0.45$*, for the rest of the parameters take the same values (see, Table. 1).*

reproduction and hence in the individual's mean density and aggregation, driving the population in the long term towards stability as seen in the figure (Fig. 5a, b).

So, in the case of slow diffusion, when competition is low, the average density of individuals takes higher values with stronger cell aggregation in the short and medium term, than in the case of intense competition (see, Fig. 5a, b & Fig. 6a, b). In the long term, the $C(r,t)$ function tends to stabilize and to reach an equilibrium characterized by an aggregative spatial structure, although the initial intensity of competition between the cells was different for the two figures (weak intensity of competition in Fig. 5b, c & Fig. 5e, f versus high intensity in Fig. 6b, c & Fig. 6e, f). We can see at equilibrium that the correlation function of the $C(r,t)$ pairs in both cases is almost identical. Hence, the competition has a striking effect in the short and medium term on the aggregation of cells, while in the long term, the population stabilizes and the effect of competition is reduced due to an equilibrium between different mechanisms that act within the population, between cell reproduction and competition on the one hand, and between the creation of aggregates and cell diffusion on the other hand.

High cell diffusion allows cells to disperse rapidly in space and to free themselves from aggregates (if the force of attraction is lower than diffusion), which reduces cluster formation, thus local density in small neighborhoods is decreased, engendering an

increase in cell reproduction and thus in the average density of individuals (see, Fig. 4a, b; Fig. 5a, b & Fig. 6a, b).

6 Discussion

In our research, we were interested in the dynamics of a population of motile phytoplankton and more specifically in the phenomenon of aggregation of these living beings. We wanted to study this phenomenon, using a new approach, called the spatial moments whose role is giving good approximation of the dynamics of individual-based models (IBM).

Based on the results obtained from our simulations, the spatial moment model gave a good prediction of the behaviour of the IBM for the selected parameters. Indeed, the two models showed rigorously the same trend in population dynamics and spatial structure where the information provided by the Clark & Evans index for IBM corresponds to that provided by the pair correlation function $C(r,t)$ for SMM. The application of the spatial moments method has allowed to build an aggregated mathematical model from small-scale biological processes characterizing phytoplankton cells and helped to analyze both the temporal evolution of the population density and the emerging spatial structure obtained when taking into account the different spatial interactions between cells. Thus, the spatial moments model obtained here can be considered in the phytoplankton literature as the first mesoscopic model developed for the study of phytoplankton aggregation in the presence of competition in the division process. It permits to explore and describe on an intermediate scale the changes (in time) that have occurred within the population.

The analysis of the simulation results of the two models leads to the conclusion that the formation of phytoplankton aggregates is due to both the attraction of cells to each other as a consequence of their chemosensory capacities and the process of cell reproduction.

In contrast with the IBM, which was long and hard to go far in time, we were able with the spatial moments model to complete the analysis, and see in the long-term the simultaneous effect of cellular diffusion and competition on individual average density and on their aggregation in the case of a large perception radius. As a result, high cell diffusion can be considered as a means of reducing and attenuating competition in the population and particularly at the level of small neighborhoods.

The deterministic approximation by moments made it possible not only to study the aggregation phenomenon and to capture the local spatial interactions of individuals due to the existence of competition for resources and chemosensory abilities in phytoplankton, but also to follow the evolution over time of the local environment of individuals and to understand the links between spatial structure and population dynamics, contrary to aggregate models of the mean-field which are unable to do so. Furthermore, the application of the spatial moments method helps to reduce the complexity of stochastic models, it is easier to analyze and minimizes the memory capacity and computing time required for simulation, especially if we are interested on the behaviour of models over the long term or on the identification of stationary states, the moment models give results more quickly and do not need high-performance computer hardware as IBM

models do. As we noticed in this study, in the simulations, with the spatial moments model we went up to $300\ days$, while for IBM it was already too much at $67\ days$. Nevertheless, the moment approximation is not without limits, this method is based on a system composed of the dynamics of the first and second spatial moment, which we are constrained to close. The choice of the closure is very important, because the use of an inappropriate closure will have an impact on the quality of the approximations, also, this method depends only on the first and the second spatial moment, it does not take into account the correlations of triplets or quadruplets ...etc, which can exist between individuals of the population.

Appendix

A The moment closure

- The power-1 closure [8, 20] is defined by:

$$T(\xi,\xi',t) = N(t)\,C(\xi,t) + N(t)\,C(\xi',t) + N(t)\,C(\xi'-\xi,t) - 2N(t)^3 \qquad (11)$$

- The power-2 closure [8, 19, 20] is defined by:

$$T(\xi,\xi',t) = \frac{1}{\alpha+\gamma}(\alpha\frac{C(\xi,t)C(\xi',t)}{N(t)} + \beta\frac{C(\xi,t)C(\xi'-\xi,t)}{N(t)} + \gamma\frac{C(\xi',t)C(\xi'-\xi,t)}{N(t)} - \beta N(t)^3) \qquad (12)$$

The symmetric power-2 closure corresponds to the case where $\alpha = \beta = \gamma$.

- The power-3 closure [16] is defined by:

$$T(\xi,\xi',t) = \frac{C(\xi,t)C(\xi',t)C(\xi'-\xi,t)}{N(t)^3} \qquad (13)$$

References

1. M. Adioui, O. Arino, and N. El Saadi. A nonlocal model of phytoplankton aggregation. *Nonlinear Analysis: Real World Applications*, 6(4):593–607, 2005.
2. W. Bell and R. Mitchell. Chemotactic and Growth Responses of Marine Bacteria to Algal Extracellular Products. *The Biological Bulletin*, 143(2):265–277, 1972.
3. B. Bolker. Analytic models for the patchy spread of plant disease. *Bulletin of Mathematical Biology*, 61(5):849–874, 1999.
4. B. Bolker and S.W. Pacala. Using Moment Equations to Understand Stochastically Driven Spatial Pattern Formation in Ecological Systems. *Theoretical Population Biology*, 52(3):179–197, 1997.
5. N. Bordj and N. El Saadi. Moment approximation of individual-based models. Application to the study of the spatial dynamics of phytoplankton populations. *Applied Mathematics and Computation*, 412:126594, January 2022.
6. P.J. Clark and F.C. Evans. Distance to nearest neighbor as a measure of spatial relationships in populations. *Ecology*, 35(4):445–453, 1954.
7. U. Dieckmann, T. Herben, and R. Law. Spatio-temporal processes in plant communities. IIASA. Working Papers, IR-97-026, 1997.

8. U. Dieckmann and R. Law. Relaxation projections and the method of moments. In U. Dieckmann, R. Law, and Johan A. J. Metz, editors, *The Geometry of Ecological Interactions*, pages 412–455. Cambridge University Press, Cambridge, 2000.
9. N. El Saadi. *Modélisation et Études Mathématique et Informatique de Populations Structurées Par Des Variables Aléatoires. : Application à l'agrégation Du Phytoplancton.* PhD Thesis, École Doctorale des Sciences Exactes et de leurs Applications, Université de Pau et des pays de l'Adour, 2004.
10. N. El Saadi and O. Arino. A stochastic modelling of phytoplankton aggregation. *Revue Africaine de la Recherche en Informatique et Mathématiques Appliquées*, 5:80–94, 2006.
11. N. El Saadi and A. Bah. On phytoplankton aggregation: A view from an IBM approach. *Comptes Rendus Biologies*, 329(9):669–678, 2006.
12. N. El Saadi and A. Bah. An individual-based model for studying the aggregation behavior in phytoplankton. *Ecological Modelling*, 204(1):193–212, 2007.
13. D.T. Gillespie. A general method for numerically simulating the stochastic time evolution of coupled chemical reactions. *Journal of Computational Physics*, 22(4):403–434, 1976.
14. V. Grimm, T. Wyszomirski, D. Aikman, and J. Uchmański. Individual-based modelling and ecological theory: Synthesis of a workshop. *Ecological Modelling*, 115(2-3):275–282, 1999.
15. G.A. Jackson. Simulation of bacterial attraction and adhesion to falling particles in an aquatic environment: Attraction to falling algae. *Limnol. Oceanogr.*, 34(3):514–530, 1989.
16. J. G. Kirkwood. Statistical mechanics of fluid mixtures. 3(5):300–313, 1935.
17. R. Law and U. Dieckmann. A Dynamical System for Neighborhoods in Plant Communities. *Ecology*, 81(8):2137–2148, 2000.
18. R. Law and U. Dieckmann. Moment approximations of individual-based models. In U. Dieckmann, R. Law, and J.A.J. Metz, editors, *The Geometry of Ecological Interactions*, pages 252–270. Cambridge University Press, Cambridge, 2000.
19. R. Law, D.J. Murrell, and U. Dieckmann. Population growth in space and time: Spatial logistic equations. *Ecology*, 84(1):252–262, 2003.
20. D.J. Murrell, U. Dieckmann, and R. Law. On moment closures for population dynamics in continuous space. *Journal of Theoretical Biology*, 229(3):421–432, 2004.
21. S.W. Pacala and S.A. Levin. Biologically generated spatial pattern and the coexistence of competing species. *Spatial ecology: the role of space in population dynamics and interspecific interactions. Princeton University Press, Princeton, NJ*, pages 204–232, 1997.
22. N. Picard and A. Franc. Approximating spatial interactions in a model of forest dynamics. *Forest Biometry, Modelling and Information Science*, 1:91–103, 2004.